



Cite this article: Zhang Y *et al.* 2022

Optogenetic manipulation of cyclic guanosine monophosphate to probe phosphodiesterase activities in megakaryocytes. *Open Biol.* **12**: 220058.

<https://doi.org/10.1098/rsob.220058>

Received: 23 February 2022

Accepted: 25 July 2022

Subject Area:

cellular biology

Keywords:

optogenetics, megakaryocytes, cGMP, phosphodiesterase

Authors for correspondence:

Shiqiang Gao

e-mail: gao.shiqiang@uni-wuerzburg.de

Markus Bender

e-mail: bender_m1@ukw.de

[†]Contributed equally.

Electronic supplementary material is available online at <https://doi.org/10.6084/m9.figshare.c.6135589>.

Optogenetic manipulation of cyclic guanosine monophosphate to probe phosphodiesterase activities in megakaryocytes

Yujing Zhang^{1,†}, Pascal Benz^{1,†}, Daniel Stehle², Shang Yang³, Hendrikje Kurz¹, Susanne Feil², Georg Nagel³, Robert Feil², Shiqiang Gao³ and Markus Bender¹

¹Institute of Experimental Biomedicine—Chair I, University Hospital and Rudolf Virchow Center, 97080 Würzburg, Germany

²Interfakultäres Institut für Biochemie, University of Tübingen, Tübingen, Baden-Württemberg, Germany

³Department of Neurophysiology, Institute of Physiology, Biocenter, University of Würzburg, 97070 Würzburg, Germany

RF, 0000-0002-7335-4841; SG, 0000-0001-6190-9443; MB, 0000-0002-2381-116X

Cyclic guanosine monophosphate (cGMP) signalling plays a fundamental role in many cell types, including platelets. cGMP has been implicated in platelet formation, but mechanistic detail about its spatio-temporal regulation in megakaryocytes (MKs) is lacking. Optogenetics is a technique which allows spatio-temporal manipulation of molecular events in living cells or organisms. We took advantage of this method and expressed a photo-activated guanylyl cyclase, *Blastocladia emersonii* Cyclase opsin (*BeCyclop*), after viral-mediated gene transfer in bone marrow (BM)-derived MKs to precisely light-modulate cGMP levels. *BeCyclop*-MKs showed a significantly increased cGMP concentration after illumination, which was strongly dependent on phosphodiesterase (PDE) 5 activity. This finding was corroborated by real-time imaging of cGMP signals which revealed that pharmacological PDE5 inhibition also potentiated nitric oxide-triggered cGMP generation in BM MKs. In summary, we established for the first-time optogenetics in primary MKs and show that PDE5 is the predominant PDE regulating cGMP levels in MKs. These findings also demonstrate that optogenetics allows for the precise manipulation of MK biology.

Highlights

- Establishment of optogenetics in primary MKs
- Illumination of YFP-*BeCyclop* megakaryocytes results in a significant cGMP increase
- Phosphodiesterase 5 hydrolyses elevated cGMP in megakaryocytes in several minutes

1. Introduction

Binding of nitric oxide (NO) to guanylyl cyclases increases the cyclic guanosine monophosphate (cGMP) formation. cGMP is a key intracellular signalling molecule in many cell types and tissues and exerts multiple cellular effects via its downstream effectors, such as protein kinase G (PKG) or cyclic nucleotide-gated channels [1]. The cGMP signalling pathway is long known for its critical role in the maintenance of cardiovascular homeostasis. Fluorescent cGMP biosensors have emerged as powerful tools for the sensitive analysis of cGMP pathways at the single-cell level [2], and methods that allow for precise

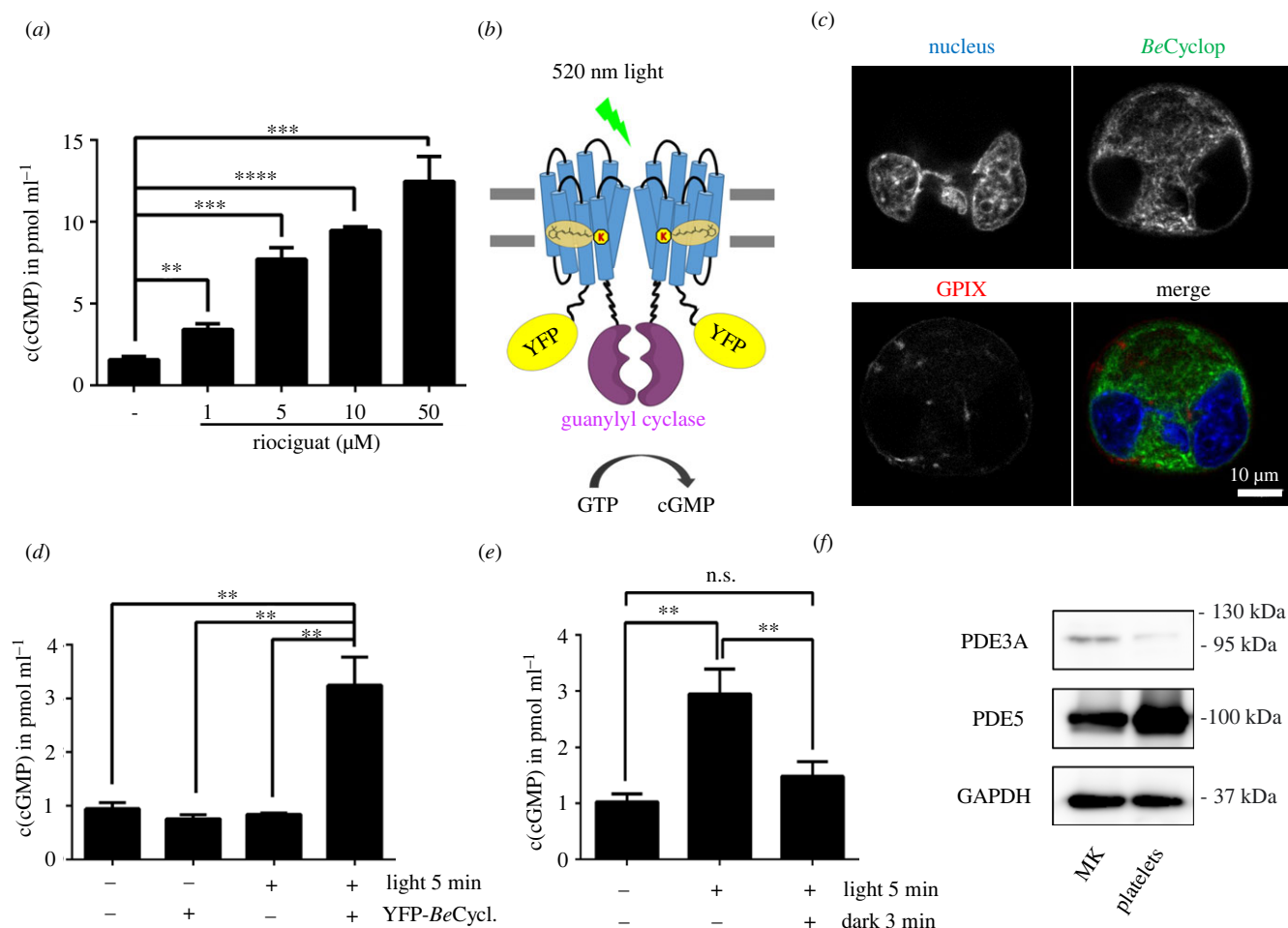


Figure 1. Optogenetic manipulation of cGMP levels in BM-derived MKs. (a) BM-derived MKs were incubated for 10 min with 1, 5, 10 or 50 μM riociguat. DMSO was used as vehicle control. ($n = 3$, representative for two independent experiments). (b) A schematic model of the light-gated guanylyl cyclase, *BeCyclop*. (c) Representative images (microscope: Leica SP8) of YFP-*BeCyclop* expression in BM-derived MKs. MK/platelet-specific membrane protein GPIIX. (d) BM-derived YFP-*BeCyclop*-expressing MKs were illuminated with green light (520 nm) for 5 min and immediately lysed. Untransduced cells or no illumination served as controls. ($n = 3$, representative for two independent experiments). (e) YFP-*BeCyclop*-expressing MKs were illuminated with green light (520 nm) for 5 min and immediately lysed or after 3 min in the dark. (f) The expression of PDE3 and PDE5 in BM-derived MKs and platelets. GAPDH served as control.

manipulation of cGMP levels by light are being developed [3]. The NO/cGMP/PKG pathway is highly expressed in platelets and its activation has been linked to platelet inhibition [4]. Analysis of spatio-temporal dynamics of platelet cGMP using cGMP sensor mice revealed that cGMP generation is increased in shear-exposed platelets at the periphery of a thrombus thereby limiting thrombus growth [5]. Cellular cGMP levels are regulated by phosphodiesterases (PDEs), which catalyse the hydrolysis of the 3' phosphate bond of cGMP to generate 5' GMP. Platelets express PDE2, 3 and 5, of which each is able to degrade cGMP [4–7]. Bone marrow (BM) megakaryocytes (MKs) are the immediate progenitor cells of blood platelets [8]. Studies on MKs derived from mouse fetal liver cells (FLCs) showed that PDE3A, PDE4A1 and PDE5 are detectable in maturing MKs, while PDE2A is found in the non-MK fraction, and that *in vitro* platelet release is enhanced by cGMP [9]. However, the spatio-temporal regulation of cGMP signals by PDEs in MKs has not been addressed due to the lack of appropriate tools. Therefore, we expressed a light-sensitive guanylyl cyclase in primary BM-derived MKs to tightly manipulate cGMP levels [3]. We demonstrate that the cGMP concentration in these MKs can be increased upon illumination, which rapidly declines in the dark caused by PDE5 activity.

2. Results and discussion

Concentration-dependent increase of cGMP in BM-derived MKs was measured when cells had been incubated with riociguat, a pharmacological stimulator of the NO-sensitive guanylyl cyclase (figure 1a). To tightly manipulate cGMP levels, the photo-activated guanylyl cyclase opsin from *Blasotocladia emersonii*, *BeCyclop* (figure 1b), was expressed in BM-derived MKs after viral transduction, which allows light-triggered cGMP increase as shown in heterologous cells and *Caenorhabditis elegans* [3]. Localization of YFP-*BeCyclop* in the membrane system of BM-derived MKs was confirmed by confocal microscopy (figure 1c). Illumination (green light: 520 nm, 5 min) of YFP-*BeCyclop*-MKs resulted in a significant increase in cGMP (3.25 ± 0.43 pmol ml⁻¹) as compared to samples in the dark (0.76 ± 0.06 pmol ml⁻¹) and untransduced cells (no light: 0.95 ± 0.09 pmol ml⁻¹; light: 0.84 ± 0.02 pmol ml⁻¹) (figure 1d). These data demonstrate that it is possible to modulate intracellular cGMP in primary MKs with optogenetic approaches. Interestingly, a rapid decrease of the intracellular cGMP concentration close to the baseline level was observed within 3 min after illumination, pointing to a high cGMP-hydrolysing PDE activity in MKs (figure 1e). We determined the expression of the

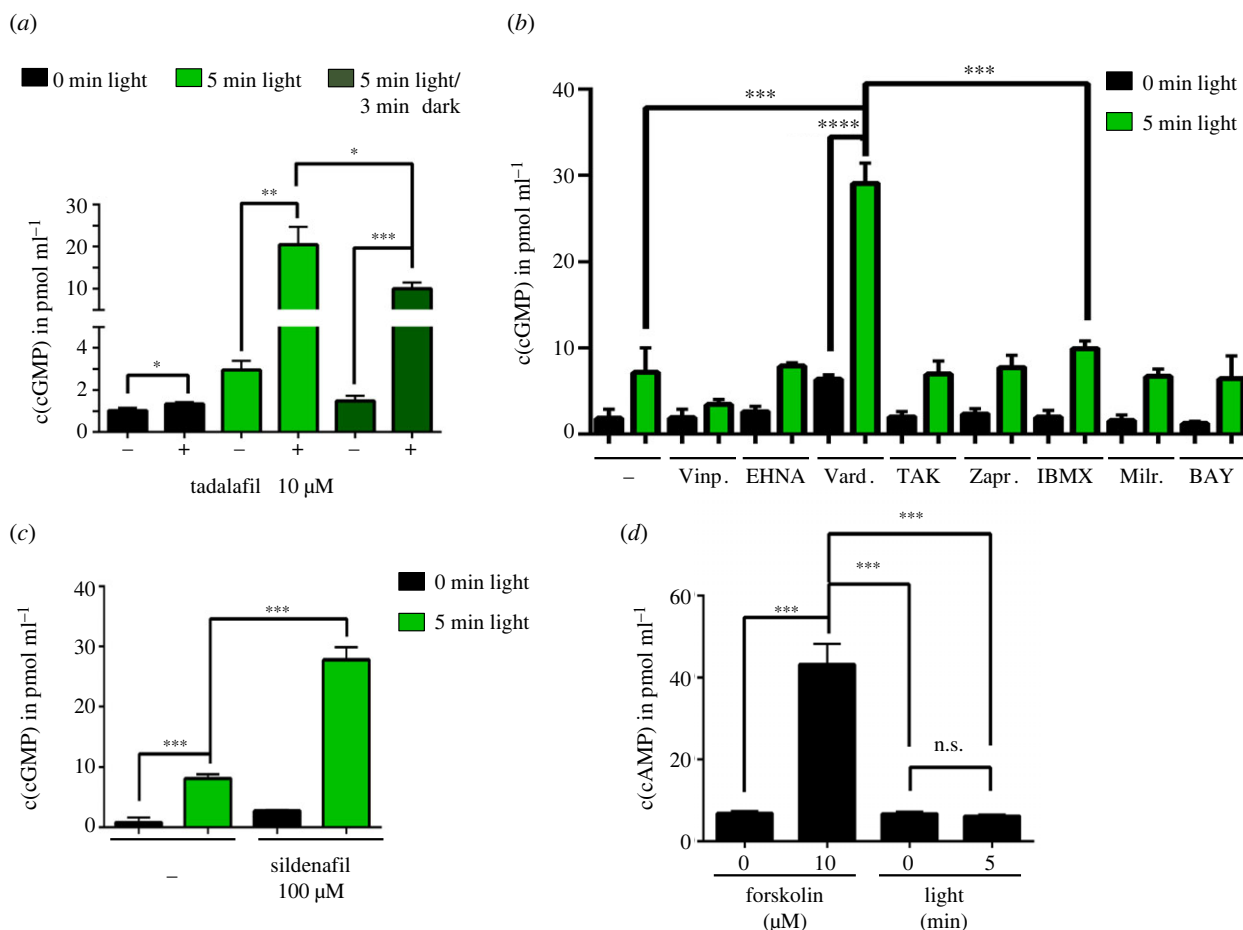


Figure 2. PDE5 regulates optogenetically increased cGMP levels in MKs. (a) BM-derived MKs were preincubated with tadalafil for 10 min prior to 5 min illumination. Cells were either lysed immediately or after 3 min before measuring cGMP concentration. ($n = 3$, representative for two independent experiments). (b,c) BM-derived MKs were preincubated with different PDE inhibitors for 10 min prior to illumination. Cells were either lysed immediately or after 3 min in the dark before measuring cGMP concentration. DMSO control in (b), H_2O control in (c). ($n = 3$). Vinpocetine (Vinp.): 20 μM , EHNA: 10 μM , vardenafil (Vard.): 50 μM , TAK-063: 0.15 μM , zaprinast (Zapr.): 40 μM , IBMX: 100 μM , milrinone (Milr.): 20 μM , BAY 60-7550: 10 μM , sildenafil: 100 μM . (d) The determination of cAMP concentration of YFP-BeCyclop-expressing BM-derived MKs after incubation with forskolin or illumination with green light for 5 min ($n = 3$).

most relevant PDEs and found a strong expression of PDE5 and only a weak expression of PDE3 in BM-derived MKs and platelets (figure 1f). This data is in agreement with the copy number analysis of the murine platelet proteome, which revealed a high PDE5 expression in murine platelets [10]. Therefore, cells were pretreated with the specific PDE5 inhibitor tadalafil, which resulted in a significant but only subtle cGMP increase (DMSO: 1.02 ± 0.15 pmol ml⁻¹; tadalafil: 1.34 ± 0.09 pmol ml⁻¹; figure 2a). However, cGMP levels were 6.9-fold increased when pretreated with tadalafil and 5 min illuminated (20.45 ± 4.3 pmol ml⁻¹), as compared to illumination without tadalafil pretreatment (2.95 ± 0.45 pmol ml⁻¹). These data strongly suggest that PDE5 limits the cGMP concentration increase in MKs. Furthermore, the inhibition of PDE5 resulted in less cGMP decrease to 10 ± 1.5 pmol ml⁻¹ in 3 min after illumination (figure 2a), again confirming that PDE5 degrades cGMP in MKs. In agreement with our findings with tadalafil, illuminated MKs preincubated with other PDE5 inhibitors (vardenafil: PDE5, 6; sildenafil: PDE5, 6) also significantly increased cGMP concentration compared to illuminated YFP-BeCyclop-MKs without inhibitor (figure 2b,c), whereas non-PDE5 inhibitors did not elevate intracellular cGMP (vinpocetine: PDE1; EHNA: PDE2; BAY60-7550: PDE2; milrinone: PDE3, 4; TAK-063: PDE10; figure 2b). Interestingly, also the broad-spectrum PDE inhibitor zaprinast (PDE5,

6, 9, 10, 11) and IBMX (PDE1, 2, 3, 4, 5, 7, 11) had no or only minor effects, respectively (figure 2b).

To demonstrate the high specificity of BeCyclop, MKs expressing YFP-BeCyclop were either stimulated with the adenylyl cyclase activator forskolin or illuminated and subsequently, cyclic adenosine monophosphate (cAMP) was determined. While forskolin significantly increased the cAMP concentration in MKs, illumination had no effect on cAMP concentration, demonstrating that BeCyclop cannot produce or influence cAMP (figure 2d).

Next, we used MK/platelet-specific cGMP sensor mice to spatio-temporally visualize cGMP dynamics in MKs *ex vivo* (figure 3a) [5,11]. Isolated femurs with externalized BM were superfused with 1 ml min⁻¹ imaging buffer. In contrast with static cell culture experiments, this method allows to rapidly add and remove the pharmacological compounds within seconds similar to optogenetic experiments. Application of the NO donor diethylamine NONOate (DEA/NO) increased cGMP in BM MKs (figure 3b,c). Similar to the optogenetic results, the PDE5-specific inhibitor tadalafil alone slowly increased cGMP and significantly augmented the NO-induced cGMP signal in MKs (figure 3b,c). These data strongly suggest that BM MKs in their native environment express a functional NO/cGMP/PDE5 signalling pathway that can be pharmacologically enhanced with PDE5 inhibitors.

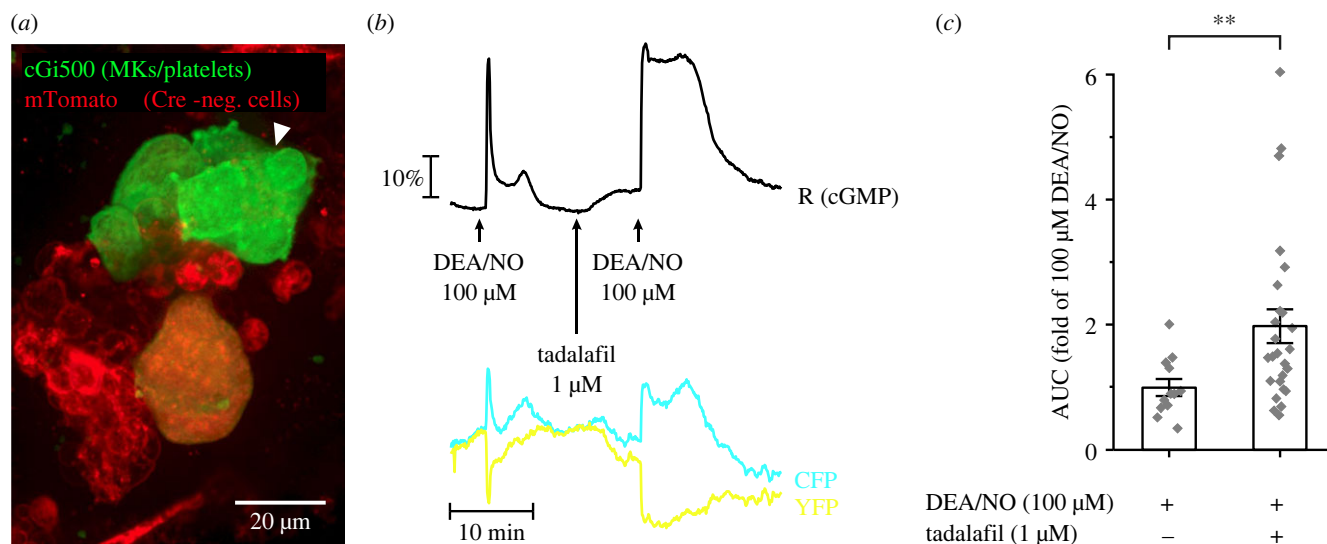


Figure 3. Real-time cGMP imaging in MKs. FRET-based cGMP imaging was performed with BM from MK/platelet-specific cGMP sensor mice. (a) Representative field of view of a measurement. Green colour indicates cGMP sensor expressing MKs. mTomato (red) is expressed in all other cells. The white arrowhead points towards the MK measured in (b). (b) Representative real-time FRET/cGMP measurement. During recording, DEA/NO (100 μM) was applied for 2 min with or without 7 min pre-incubation with tadafafil (1 μM). Black trace represents the CFP/YFP ratio R , which indicates cGMP concentration changes. Relative fluorescence changes of the individual fluorescent proteins are shown as cyan (CFP) and yellow (YFP) trace. (c) Statistical analysis was performed with the AUC of cGMP signals induced by DEA/NO (100 μM) in the presence of tadafafil (1 μM) or vehicle (DMSO; 0.002%). Data represent mean \pm s.e.m. of $n \geq 12$ MKs from greater than or equal to three mice. Scale bar, 20 μm .

Optogenetics has become successful as an easily applicable tool for precise spatio-temporal manipulation of molecular events in living cells or organisms. By now, optogenetic applications have expanded from neuroscience to other fields such as the cardiovascular system. We established to the best of our knowledge the first-time optogenetics in primary MKs. By expressing the photo-activated guanylyl cyclase, *BeCyclop*, we tightly controlled cGMP levels in MKs by light. We show that PDE5 is the major PDE, counteracting cGMP levels in BM-derived MKs, and could verify our optogenetic results by cGMP imaging in BM MKs *ex vivo* using cGMP sensor mice. Our reversible approaches allowing to trigger the intracellular process and directly analyse the effect in a high spatio-temporal resolution revealed that PDE5 is highly active in BM-derived MKs as cGMP levels rapidly declined after removing the stimulus. Our findings are corroborated by research on mouse FLC-derived MKs showing that PDE5 expression is highest in mature FLC-derived MKs [9]. Our study shows that optogenetics in MKs allows to light-modulate the function of key signalling molecules thereby possibly identifying novel regulatory mechanisms of MK maturation and platelet production. However, our study has also limitations as the transduction efficiency of MKs was only about 30%. We analysed the complete MK fraction since complicated sorting of mature MKs (cell diameter of approx. 35 μm) probably leads to light-activation before starting the experiment. Thus, our data even underestimate the light-induced increase of cGMP in single MKs expressing YFP-*BeCyclop* due to the untransduced cell fraction. Further studies are required using MK/platelet-specific optogenetic mouse lines to spatio-temporally light-manipulate molecules or proteins in MKs and platelets *in vivo*. The finding that BM MK express PDE5 also informs future therapeutic strategies to increase cGMP concentrations and potentially modulate platelet biogenesis with clinically used PDE5 inhibitors.

3. Experimental procedures

3.1. Animals

MK/platelet-specific cGMP sensor mice (*cGi500-L2^{fl/fl}; Pfa-Cre^{tg/tg}* [12]) were used to visualize cGMP signals in MKs in real time [5,11]. Mouse BM isolation was conducted according to the guidelines of the local governments.

3.2. Reagents

Riociguat (Selleck Chemicals), tadafafil (Sigma-Aldrich/Supelco), DMSO, forskolin (Sigma-Aldrich), vinpocetine, EHNA (Enzo Life Sciences), BAY60-7550, TAK-063 (Cayman Chemical), milrinone, vardenafil, zaprinast (Santa Cruz Biotechnology), sildenafil (Merck), IBMX (Thermo Fisher Scientific) and DEA/NO (Axxora).

3.3. Bone marrow-derived megakaryocytes

BM cells were obtained from femur and tibia of C57BL/6 mice by flushing, and lineage depletion was performed using an antibody cocktail of anti-mouse CD3, clone 17A2; anti-mouse Ly-6G/Ly-6C, clone RB6-8C5; anti-mouse CD11b, clone M1/70; anti-mouse CD45R/B220, clone RA3-6B2; anti-mouse TER-119/Erythroid cells, clone Ter-119 (1.5 μg of each antibody per mouse, Biologend) and magnetic beads (Dynabeads Untouched Mouse CD4 Cells, Invitrogen). Lineage-negative (Lin-) cells were cultured in DMEM medium (supplemented with 4 mM L-glutamine, 100 U ml⁻¹ penicillin, 50 mg ml⁻¹ streptomycin) containing 1% of recombinant TPO (homemade) and 100 U ml⁻¹ recombinant Hirudin (Hyphen Biomed) at 37°C under 5% CO₂.

3.4. Expression of YFP-*BeCyclop* in megakaryocytes

YFP-*BeCyclop* DNA was cloned into the murine stem cell virus vector and transfected into 293T cells. Viral supernatant

was collected and BM-derived cells were infected on day 1 [13]. A bovine serum albumin density gradient was used at culture day 3 to separate MKs from non-MK cells. Experiments were performed on day 4.

3.5. Illumination and determination of cyclic guanosine monophosphate concentration

Cell density was adjusted to 5×10^4 cells ml^{-1} . If needed, samples were preincubated with agonist or inhibitor for 10 min at room temperature. Subsequently, samples were kept in the dark or illuminated with light (520 nm, 20 $\mu\text{W mm}^{-2}$) for 5 min at room temperature and lysed either immediately or after 3 min in the dark with 0.1 M hydrogen chloride. Concentrations of cGMP or cAMP were measured by DetectX Direct cyclic GMP or AMP Enzyme Immunoassay Kit, respectively, and analysed by the optical density at 450 nm with a Thermo Scientific Multiskan microplate spectrophotometer.

3.6. Immunoblotting

MK and platelet lysates were separated by sodium dodecyl sulfate-polyacrylamide gel electrophoresis and blotted onto polyvinylidene difluoride membranes. Membranes were incubated with an anti-PDE3A antibody (GeneTex) or an anti-PDE5 antibody (Abcam) overnight. Horseradish peroxidase-conjugated secondary antibodies and enhanced chemiluminescence solution (MoBiTec) were used for visualization. Immunoblots were recorded directly using an Amersham Imager 600 (GE Healthcare).

3.7. Real-time cyclic guanosine monophosphate imaging in megakaryocytes *ex vivo*

Femurs and tibias were dissected from MK/platelet-specific cGMP sensor mice (*cGi500-L2^{fl/fl}; Pfa-Cre^{tg/tg}* [12]). Bone tissue was carefully removed with scissor and forceps on one side to give access to the BM. Opened bones were placed in a superfusion chamber (RC 26, Warner Instruments), mounted with a Slice Hold-Down (SHD 26H/10, Warner Instruments) and continuously superfused with imaging buffer (140 mM NaCl, 5 mM KCl, 1.2 mM MgCl_2 , 2 mM

CaCl_2 , 5 mM HEPES and 10 mM D-glucose; pH = 7.4) with or without added drugs. Real-time FRET/cGMP imaging was performed by recording CFP and YFP fluorescence as described in detail elsewhere [14]. The relative CFP/YFP ratio change (black trace in the respective graph; referred to as R (cGMP)) correlates with the cGMP concentration change.

3.8. Data analysis

Results are shown as mean \pm s.e.m. Statistical significance was assessed by an unpaired *t*-test with GraphPad Prism software. *p*-values < 0.05 were considered significant (**** < 0.0001; *** < 0.001; ** 0.001 to 0.01; * 0.01 to 0.05). ns: non-significant. Statistical analysis of cGMP sensor imaging data was performed with Origin 2019 (OriginLab, Northampton, MA, USA). Since datasets were not normally distributed, statistical differences were analysed non-parametrically by Mann-Whitney *U*-test.

Ethics. Mouse bone marrow isolation was conducted according to the guidelines of the local governments.

Data accessibility. Any additional information required to reanalyse the data reported in this paper is available from the corresponding author upon request.

Authors' contributions. Y.Z.: data curation, investigation, methodology and writing—review and editing; P.B.: data curation, investigation, methodology and writing—review and editing; D.S.: data curation, investigation, methodology and writing—review and editing; S.Y.: data curation and methodology; H.K.: investigation and methodology; S.F.: funding acquisition, investigation, methodology, supervision and writing—review and editing; G.N.: funding acquisition, methodology, project administration, supervision and writing—review and editing; R.F.: funding acquisition, project administration, supervision and writing—review and editing; S.G.: funding acquisition, project administration, supervision and writing—original draft; M.B.: conceptualization, funding acquisition, project administration, supervision and writing—original draft.

All authors gave final approval for publication and agreed to be held accountable for the work performed therein.

Conflict of interest declaration. We declare we have no competing interests.

Funding. This work was supported by TR240 grant with project no. 374031971 of the Deutsche Forschungsgemeinschaft (DFG; German Research Foundation).

Acknowledgements. The authors thank Sarah Seidel and Dr Markus Spindler for the help with experiments.

References

- Friebe A, Sandner P, Schmidt A. 2020 cGMP: a unique 2nd messenger molecule - recent developments in cGMP research and development. *Naunyn Schmiedebergs Arch. Pharmacol.* **393**, 287–302. (doi:10.1007/s00210-019-01779-z)
- Feil R, Lehnert M, Stehle D, Feil S. 2021 Visualising and understanding cGMP signals in the cardiovascular system. *Br. J. Pharmacol.* **179**, 2394–2412. (doi:10.1111/bph.15500)
- Gao S, Nagpal J, Schneider MW, Kozjak-Pavlovic V, Nagel G, Gottschalk A. 2015 Optogenetic manipulation of cGMP in cells and animals by the tightly light-regulated guanylyl-cyclase opsin CyclOp. *Nat. Commun.* **6**, 8046. (doi:10.1038/ncomms9046)
- Walter U, Gambaryan S. 2009 cGMP and cGMP-dependent protein kinase in platelets and blood cells. *Handb. Exp. Pharmacol.* **2009**, 533–548.
- Wen L *et al.* 2018 A shear-dependent NO-cGMP-cGKI cascade in platelets acts as an auto-regulatory brake of thrombosis. *Nat. Commun.* **9**, 4301. (doi:10.1038/s41467-018-06638-8)
- Gresele P, Momi S, Falcinelli E. 2011 Anti-platelet therapy: phosphodiesterase inhibitors. *Br. J. Clin. Pharmacol.* **72**, 634–646. (doi:10.1111/j.1365-2125.2011.04034.x)
- Rondina MT, Weyrich AS. 2012 Targeting phosphodiesterases in anti-platelet therapy. *Handb. Exp. Pharmacol.* **2012**, 225–238.
- Machlus KR, Italiano Jr JE. 2013 The incredible journey: from megakaryocyte development to platelet formation. *J. Cell Biol.* **201**, 785–796. (doi:10.1083/jcb.201304054)
- Begonja AJ, Gambaryan S, Schulze H, Patel-Hett S, Italiano Jr JE, Hartwig JH, Walter U. 2013 Differential roles of cAMP and cGMP in megakaryocyte maturation and platelet biogenesis. *Exp. Hematol.* **41**, 91–101 e104. (doi:10.1016/j.exphem.2012.09.001)
- Zeiler M, Moser M, Mann M. 2014 Copy number analysis of the murine platelet proteome spanning the complete abundance range. *Mol. Cell Proteomics* **13**, 3435–3445. (doi:10.1074/mcp.M114.038513)

11. Thunemann M *et al.* 2013 Transgenic mice for cGMP imaging. *Circ. Res.* **113**, 365–371. (doi:10.1161/CIRCRESAHA.113.301063)
12. Tiedt R, Schomber T, Hao-Shen H, Skoda RC. 2007 Pf4-Cre transgenic mice allow the generation of lineage-restricted gene knockouts for studying megakaryocyte and platelet function *in vivo*. *Blood* **109**, 1503–1506. (doi:10.1182/blood-2006-04-020362)
13. Bender M, Thon JN, Ehrlicher AJ, Wu S, Mazutis L, Deschmann E, Sola-Visner M, Italiano JE, Hartwig JH. 2015 Microtubule sliding drives proplatelet elongation and is dependent on cytoplasmic dynein. *Blood* **125**, 860–868. (doi:10.1182/blood-2014-09-600858)
14. Stehle D *et al.* 2021 Novel soluble guanylyl cyclase activators increase glomerular cGMP, induce vasodilation and improve blood flow in the murine kidney. *Br. J. Pharmacol.* **179**, 2476–2489. (doi:10.1111/bph.15586)